



Triggering with the LHCb calorimeters

R. Lefevre

► To cite this version:

R. Lefevre. Triggering with the LHCb calorimeters. XIII International Conference on Calorimetry in High Energy Physics (CALOR 2008), May 2008, Pavia, Italy. 8 p. in2p3-00336000

HAL Id: in2p3-00336000

<https://hal.in2p3.fr/in2p3-00336000>

Submitted on 31 Oct 2008

HAL is a multi-disciplinary open access archive for the deposit and dissemination of scientific research documents, whether they are published or not. The documents may come from teaching and research institutions in France or abroad, or from public or private research centers.

L'archive ouverte pluridisciplinaire **HAL**, est destinée au dépôt et à la diffusion de documents scientifiques de niveau recherche, publiés ou non, émanant des établissements d'enseignement et de recherche français ou étrangers, des laboratoires publics ou privés.

Triggering with the LHCb calorimeters

Régis Lefèvre on behalf of the LHCb Collaboration

Laboratoire de Physique Corpusculaire, Université Blaise Pascal - IN2P3/CNRS, 24 avenue des Landais, 63177 Aubière Cedex, France

E-mail: lefevre@clermont.in2p3.fr

Abstract. The LHCb experiment at the LHC has been conceived to pursue high precision studies of CP violation and rare phenomena in b hadron decays. The online selection is crucial in LHCb and relies on the calorimeters to trigger on high transverse energy electrons, photons, π^0 and hadrons. In this purpose a dedicated electronic has been realized. The calorimeter trigger system has been commissioned and is used to trigger on cosmic muons before beams start circulating in the LHC. When the LHC will start, it will also provide a very useful interaction trigger.

1. Introduction

The LHCb experiment [1] is dedicated to extensive, high precision studies of CP violation and rare decays in b -flavoured hadrons. As shown in figure 1, the $b\bar{b}$ pair production at the LHC is forward peak so LHCb has been designed as a single-arm forward spectrometer to reduce the cost. Figure 2 shows the layout of the experiment which covers polar angles from 10 to 300 (250) mrad in the bending (non-bending) plane. While the Vertex Locator and the tracking system (TT, T1-T3) provide very good vertexing and tracking capabilities, excellent particle identification is achieved thanks to two ring imaging Cherenkov detectors (RICH1 and RICH2), to the calorimeters (SPD/PS, ECAL and HCAL) and to five muon stations (M1-M5).

LHCb will benefit of the large $b\bar{b}$ cross section at the LHC ($\sim 500 \mu\text{b}$). It will be operated at luminosities limited to few $10^{32} \text{ cm}^{-2}\text{s}^{-1}$ in order to maximize the probability of single interaction per crossing, facilitating the trigger and the reconstruction. At such luminosities the $b\bar{b}$ production rate is around 100 kHz but, with small branching ratios, interesting B decays in the acceptance typically correspond to rates smaller than few Hz and a powerful trigger system is required to select them.

2. Trigger Strategy

The LHCb trigger strategy relies on a large output bandwidth of 2 kHz achievable thanks to a relatively small event size (~ 35 kbytes). 200 Hz will be dedicated to exclusive selections of B candidates in specific final states for the core physic program but also for tagging efficiencies studies using self-tagged final states. The remaining 1800 Hz will be divided among three inclusive samples: a single muon sample for trigger efficiencies and data mining, an high mass di-muon sample for proper time resolution studies as well as alignment and momentum calibrations, and an inclusive D^* sample to measure particle identification performances and for charm physics.

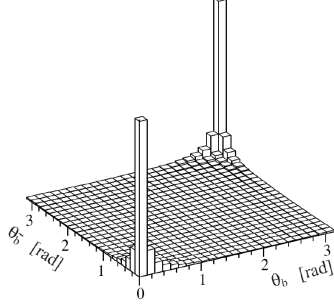


Figure 1. Polar angles of the b and \bar{b} hadrons in $b\bar{b}$ events produced in proton-proton collisions at $\sqrt{s} = 14$ TeV.

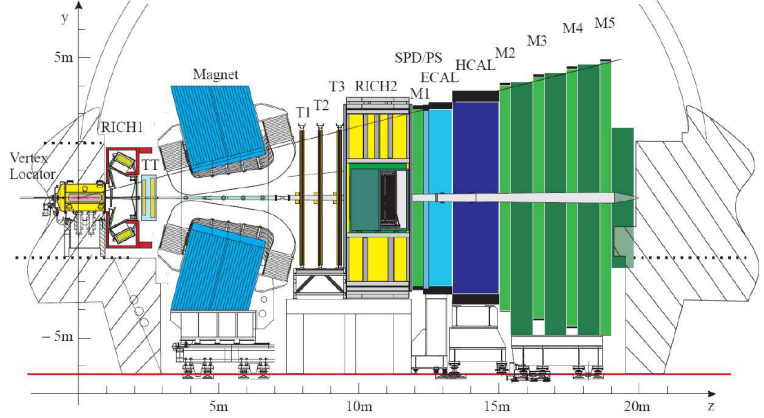


Figure 2. Layout of the LHCb spectrometer.

The LHCb trigger fully exploits the topology of B decays characterised by significant transverse momentum due to the high b quark mass and by long lifetime. To reduce the rate from the 40 MHz input of the LHC clock to the 2 kHz output to the data acquisition (DAQ), the trigger is divided in two levels. The first level, called Level 0, is implemented in custom electronic boards working in a fully synchronous architecture. It has a fixed latency of $4 \mu\text{s}$ and an output rate of 1 MHz. The second level, called High Level Trigger (HLT), uses a farm of about 2000 central processing units.

The Level 0 consists of four subsystems: the pile-up system, part of the Vertex Locator and used to veto events with more than one interaction and events with very high charged multiplicity; the calorimeter trigger which provides high transverse energy (E_T) electron, photon, π^0 and hadron candidates; the muon system which provides high transverse momentum muon and di-muon candidates; and the Level 0 Decision Unit (L0DU) which takes the decision combining the data of the three over subsystems.

The HLT first reduces the rate to something like 30 kHz using the tracking information to confirm the Level 0 candidate, eventually adding an impact parameter cut. Only then inclusive and exclusive selections are built using the full event reconstruction. Even if the calorimeters also participate to the HLT, their most critical contribution is to the Level 0 for which a dedicated electronic had to be designed, built and commissioned.

3. LHCb Calorimeters

The LHCb calorimeter system [2] is made of four consecutive semi-projective detectors shown on figure 3. The scintillating pad detector (SPD) and the preshower (PS) are two 15 mm thick scintillator planes separated by a 2.5 radiation length lead converter. The light is collected by wavelength-shifting (WLS) fibres inserted and glued in round grooves made in the square pads. The WLS fibres are connected at both ends to clear fibres that transmit the signal to multi-anode photomultipliers. The electromagnetic calorimeter (ECAL) has a shashlik sampling structure with alternating scintillating tiles and lead plates. WLS fibres penetrate the lead/scintillator stack through holes and are read out by photomultipliers. The ECAL is made of about 6000 cells with a transverse size varying from $4 \times 4 \text{ cm}^2$ close to the beam pipe, to 6×6 and $12 \times 12 \text{ cm}^2$ at larger polar angles, corresponding to one to three Moliere radius. The cell granularity is the same in the SPD and PS for a combined use in $\gamma/e/\pi$ separation. The ECAL accounts for 25 radiation lengths and 1.1 interaction lengths. The hadronic calorimeter (HCAL) consists of thin

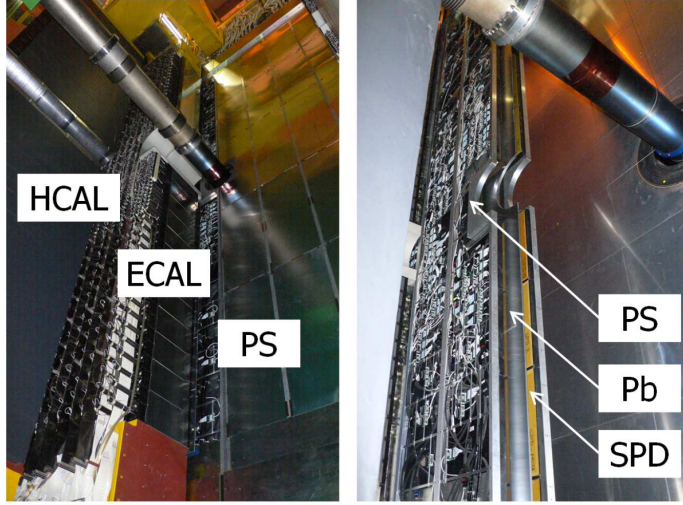


Figure 3. Pictures of the calorimeters in LHCb cavern. The transverse dimensions of the calorimeters are about 8 m horizontally and 6.5 m vertically.

iron plates interspaced with scintillating tiles arranged along the beam axis. WLS fibres run along the edges of the scintillating tiles and collect the signal to photomultipliers. The HCAL has about 1500 readout cells with a transverse size of 13×13 and 26×26 cm² in the inner and outer parts respectively. The HCAL depth is 5.6 interaction lengths.

The purpose of the LHCb calorimeter system is twofold. It gives a fast identification of high E_T electrons, photons, π^0 and hadrons making a crucial contribution to the Level 0 trigger as already mentioned. Offline and in the HLT, it significantly contributes to the electron identification and provides precise measurements of prompt photons, π^0 and η .

4. Calorimeter trigger system

The calorimeter trigger [3] relies on the E_T measurements in ECAL and HCAL clusters made of 2×2 cells. The SPD and the preshower are used to identify respectively the charged and the electromagnetic nature of the cluster. Five types of candidates are then built: electron, photon, local π^0 , global π^0 , and hadron. The local π^0 candidate corresponds to two photons on the same front-end board and is obtained as the E_T sum of the board (4×8 cells). The global π^0 candidate corresponds to two photons on neighbouring boards and is obtained by adding the highest E_T clusters of two vertically adjacent boards. The highest E_T candidate of each type is selected and send to the L0DU where different thresholds, specific to each type of candidate, are applied to eventually trigger a positive decision. The calorimeter system also provides the total SPD hit multiplicity and the total E_T , two global inputs used to veto respectively very busy events and muon halo background.

Figure 4 shows the global architecture of the calorimeter trigger system. While the selection boards and the L0DU are located in a barrack behind a concrete wall, the calorimeter crates are on a platform on top of the calorimeters in a high radiation area. Thus, anti-fuse and flash FPGAs are used, registers are protected by triple voting, and the data contain parity bits. The total processing time from the input of the front-end board to the input of the L0DU, not counting the optical transmission from the calorimeter platform to the barrack, is around 1 μ s.

Figure 5 shows the data flow in the calorimeter crates. In addition to the PS, ECAL and HCAL front-end boards, the crates contain boards dedicated to the trigger processing, namely the SPD multiplicity boards and the Trigger Validation Boards (TVB). Each crate also contains a Calorimeter Read Out Controller board (CROC) dedicated to the interface with the Experiment Control System (ECS) [4] and the DAQ. A specific backplane permits the necessary point to point transmissions between boards within the same crate via the backplane itself or in different

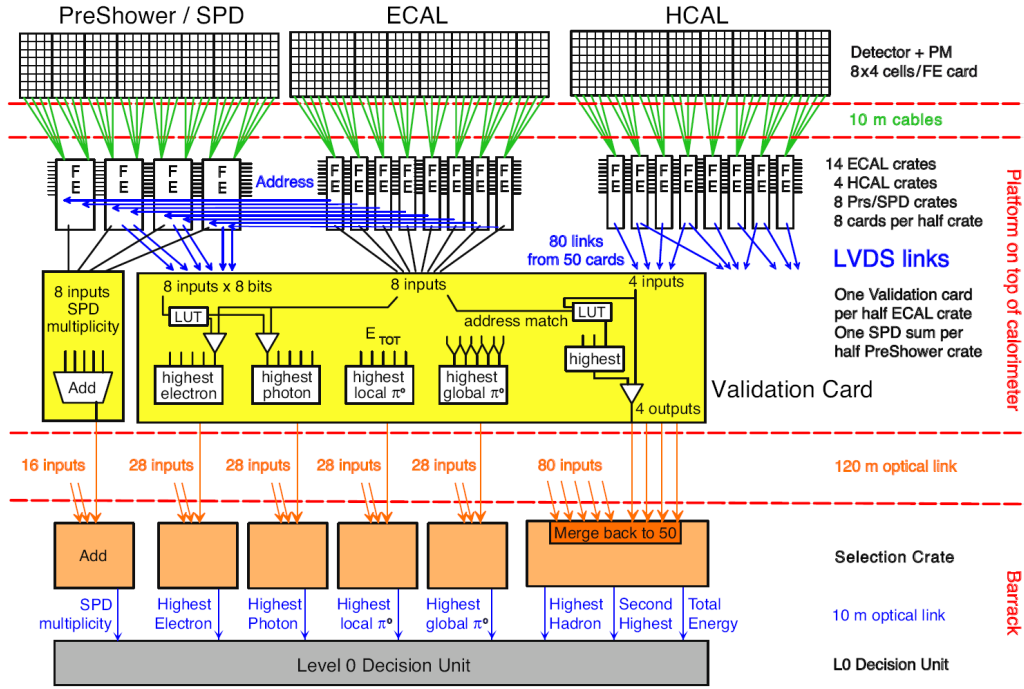


Figure 4. Architecture of the calorimeter trigger system.

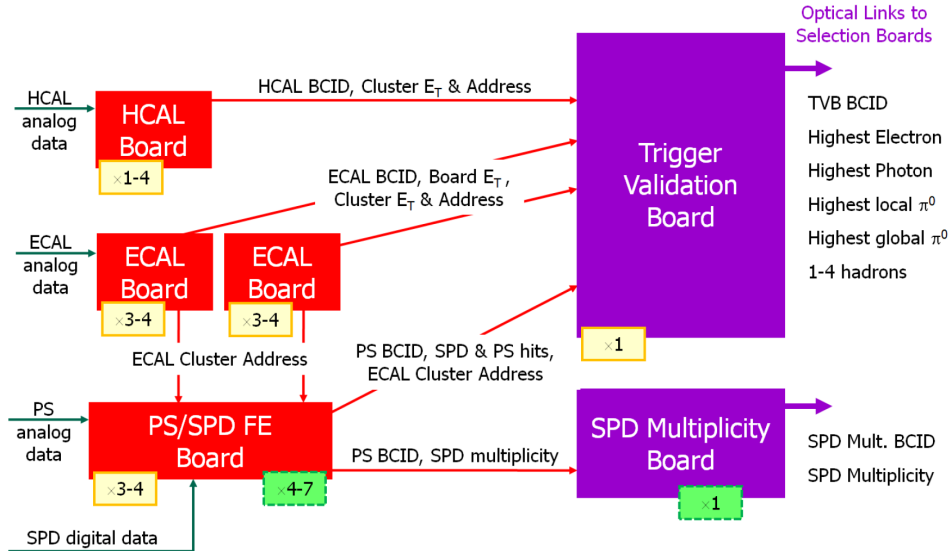


Figure 5. Trigger path data flow in the calorimeter crates. One has three or four PS/SPD front-end boards (64 SPD and 64 PS channels each), six or eight ECAL boards (32 channels each), and one to four HCAL boards (32 channels each) for each TVB. There are 28 TVB in total. One has four or seven PS/SPD boards for each SPD multiplicity board and 16 SPD multiplicity boards in total.

crates via LVDS links. It also permits the transmission of the bottom, left, and bottom-left cells respectively to the bottom, left, and bottom-left neighbour boards in order to build the 2×2 clusters at the edge of several boards.

While ECAL and HCAL front-end boards directly receive the signal from the photomultipliers, the data from the PS and the SPD are first integrated on very front-end boards. In the case of the SPD, the very front-end ASIC also corrects the data for spill-over and makes a 1-bit digitization. ECAL and HCAL front-end boards evaluate all the 2×2 clusters. Each board identifies its highest E_T cluster and sends it to the TVB. Each ECAL board also computes the board E_T summing up its 32 cells and sends it to the TVB. It also sends the address of its highest E_T cluster to the PS/SPD front-end board which sends the corresponding SPD and PS hits to the TVB. In addition, the PS/SPD board computes the number of SPD hits and sends the sum to the SPD multiplicity board.

The TVB uses the SPD and PS hits to identify electron and photon clusters within the ECAL clusters. The highest E_T electron and photon are then sent to the selection boards. The local π^0 and global π^0 candidates are respectively obtained as the highest ECAL board E_T and as the highest sum of two clusters coming from vertically adjacent ECAL boards. For each HCAL candidate, matching ECAL clusters are looked for comparing the addresses. The E_T of the matched ECAL cluster with the highest E_T is then added to the HCAL candidate in order to improve the hadron energy estimate. All the hadron candidates are then sent to the selection boards. The SPD multiplicity board sums the SPD multiplicity over the PS/SPD boards and sends it to the selection boards.

The selection boards find the highest E_T candidate of each type and sum the SPD multiplicity over the SPD multiplicity boards. They also compute the total E_T summing over the E_T of the hadron candidates from the TVB after removing duplicates related to the fact that, in order to search for matched ECAL clusters, over the fifty HCAL front-end boards thirty send their candidates to two TVB. The selection boards send their outputs to the L0DU which centralizes the Level 0 information and takes the decision. Another important part for the trigger system is the TFC (Timing and Fast Control) [5] which broadcasts the clock as well as the triggers to the front-end boards.

5. Expected performances

The Level 0 thresholds have been tuned to maximize the trigger efficiency on signal events passing the offline selection using few mainstream modes such as $B_s \rightarrow D_s^- (K^+ K^- \pi^-) K^+$, $B^0 \rightarrow J/\psi (\mu^+ \mu^-) K_s (\pi^+ \pi^-)$, $B^0 \rightarrow J/\psi (e^+ e^-) K_s (\pi^+ \pi^-)$ or $B^0 \rightarrow K^* (K^+ \pi^-) \gamma$. The 1 MHz output bandwidth of the Level 0 is dominated by the hadronic trigger with an allocated bandwidth of 700 kHz while the inclusive bandwidths for the electromagnetic (electron, photon

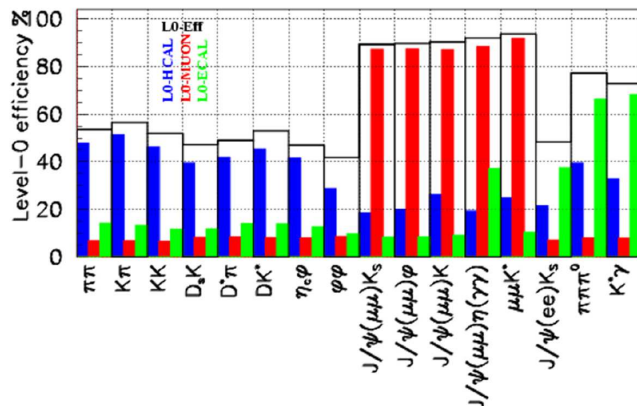


Figure 6. Level 0 efficiencies for some typical B decays. For each mode, the overall efficiency is reported as well as the inclusive efficiencies of the hadronic, muonic and electromagnetic triggers.

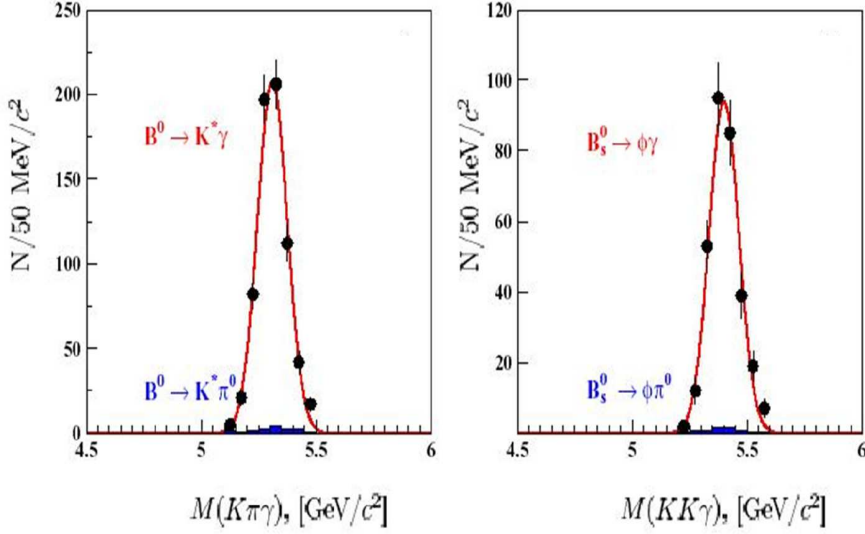


Figure 7. Reconstructed mass of the B meson in $B^0 \rightarrow K^*\gamma$ events (left) and in $B_s \rightarrow \phi\gamma$ events (right). The small background contributions respectively from $B^0 \rightarrow K^*\pi^0$ and $B_s \rightarrow \phi\pi^0$ decays are indicated.

and π^0) and muonic triggers are respectively 280 kHz and 160 kHz. Figure 6 shows some typical Level 0 efficiencies which are around 50%, 70% and 90% respectively for hadronic, electromagnetic and muonic B decays.

Essential to the first level trigger, the calorimeters also have an important contribution to the offline reconstruction providing for instance precise measurements of photons and π^0 's [6]. Figure 7 illustrates the LHCb physics potential with prompt photons on radiative B decays. It shows the reconstructed mass of the B^0 and B_s respectively in $B^0 \rightarrow K^*\gamma$ and $B_s \rightarrow \phi\gamma$ events. The expected resolution on the B meson mass is $65 \text{ MeV}/c^2$. In the $B^0 \rightarrow K^*\gamma$ ($B_s \rightarrow \phi\gamma$) mode, the expected yield for 2 fb^{-1} is $35 \cdot 10^3$ ($9 \cdot 10^3$) selected signal events with a background over signal ratio lower than 0.7 (2.9) at 90% of confidence level [7].

As for photons, the π^0 reconstruction is based on ECAL energy deposits clustered around local maxima [8]. Low transverse momenta π^0 's are mostly reconstructed as a *resolved* pair of well separated photons. At higher momenta, the distance between the two photons at the entrance of the calorimeters becomes of the order of the size of one ECAL pad and energetic π^0 's often lead to a single cluster. In order to identify those so called *merged* π^0 , an iterative procedure is used to build two virtual interleaved sub-clusters sharing the cell energies according to the expected transverse shape of photon showers. Figure 8 shows the reconstructed mass of resolved and merged π^0 candidates in $B^0 \rightarrow \pi^+\pi^-\pi^0$ events. At the π^0 mass, true π^0 's represent about one fourth of the resolved π^0 candidates which suffer from a large combinatorial background and about one half of the merged π^0 candidates. Resolved π^0 's are reconstructed with a mass resolution of around $10 \text{ MeV}/c^2$ while a core mass resolution of about $15 \text{ MeV}/c^2$ is obtained for merged π^0 's. Because of their intrinsic large transverse momentum, merged π^0 's are of major importance for the reconstruction of π^0 's from B decays. In $B^0 \rightarrow \pi^+\pi^-\pi^0$ events, the π^0 's from the B^0 meson represent only around one eighth of the true resolved π^0 's but more than half of the true merged π^0 's. In those events, the average reconstruction efficiency of the π^0 from the B^0 decay is 53% and the expected resolution on the B^0 mass is about $80 \text{ MeV}/c^2$. Those performances lead to an expected precision of 10° in the determination of the CKM angle α for 2 fb^{-1} [9] through a time dependent Dalitz analysis of $B^0 \rightarrow \rho\pi$ decays [10].

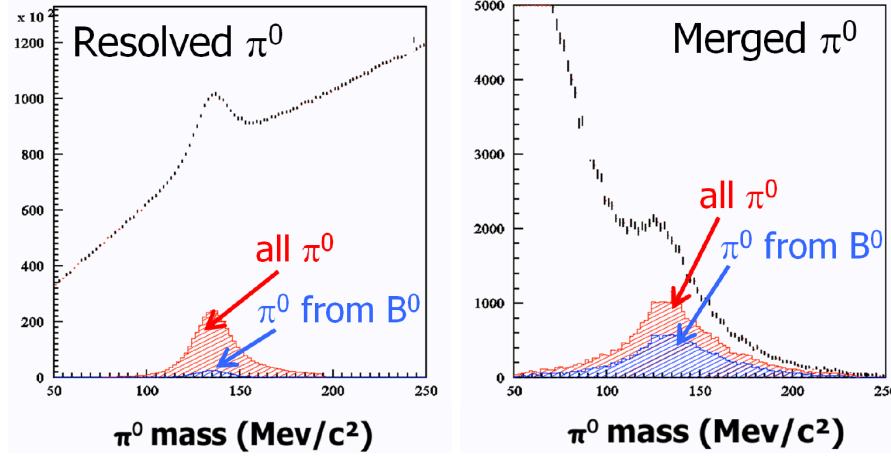


Figure 8. Reconstructed mass of resolved (left) and merged (right) π^0 candidates in $B^0 \rightarrow \pi^+\pi^-\pi^0$ events.

6. Commissioning

The commissioning of the calorimeter trigger system started in early 2007. The first in situ test of the full trigger chain was done in May 2007 as follows. First the TFC was configured by ECS to send calibration pulses used to drive the calorimeter LEDs. The front-end boards were reading out the detector and computing the trigger data at 40 MHz. Sequentially, the TVB, the selection boards and the L0DU were receiving their inputs from the previous step, making their computations and sending their outputs to the next step. The LED calibration pulses were associated to high E_T candidates in the L0DU which then sent positive trigger decisions to the TFC. Finally, the TFC broadcast the trigger to the front-end boards which sent the data, via the CROC, to the DAQ for monitoring in the control room and persistent storage. The test was fully successful and gave great confidence in the full trigger chain.

Since December 2007, the calorimeters provide a cosmic trigger to the experiment. This trigger is based on a coincidence between ECAL and HCAL with a special high voltage setting used to detect minimum ionizing particles by increasing the photomultiplier gains. This trigger has a high purity, close to 90%, and a rate of about 10 Hz. It is very useful to experience real data taking, to check cabling and mappings, and for timing and alignment studies. Figures 9 and 10 show two examples of cosmic events selected by this trigger. In the first picture, one can see, in the plan perpendicular to the beam axis, the cosmic track reconstructed in the calorimeters with hits in the SPD, the PS, the ECAL and the HCAL. In the second picture, one has, in the plane containing the beam and vertical axes, the hits left in ECAL and HCAL but also in the muon stations M2 to M5.

7. Triggers at the LHC start-up

Three kinds of trigger are foreseen for the very first collision data: a zero bias trigger, an interaction trigger and an inclusive muon trigger. The zero bias trigger will be based on the LHC bunch structure and will have to be heavily prescaled relatively early: asking for colliding bunches in LHCb will lead to rates of 214 kHz and 765 kHz respectively in the “43” and “156” LHC schemes envisaged for 2008.

This prescaled random trigger will be complemented by an interaction trigger based on some minimal activity in the calorimeters. Few solutions are being investigated and for the moment the best variable seems to be the E_T of the hadron candidate. For instance, for a cut at 1 GeV,

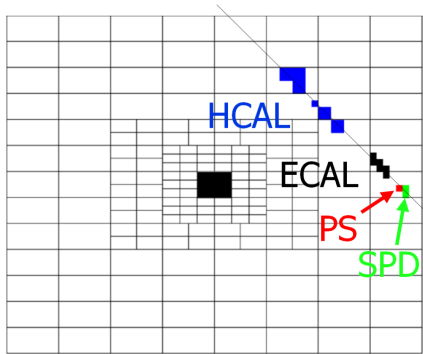


Figure 9. Hits left by a cosmic muon in the calorimeters.

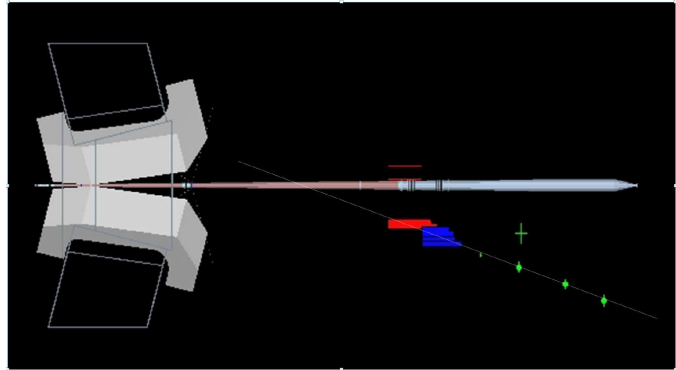


Figure 10. Hits left by a cosmic muon in ECAL and HCAL as well as in the muon stations M2 to M5.

the noise level would be very low, around 1 Hz, but the efficiencies would already be rather good: 79% for hard interactions and 97% for inclusive B production.

8. Conclusion

In the LHCb experiment, the trigger is a key point and heavily relies on the calorimeters. More than 80% of the first level trigger output bandwidth will be dedicated to high E_T electron, photon, π^0 and hadron candidates identified by the calorimeter trigger system. This system has been commissioned and is now routinely used to trigger on cosmic tracks. Thanks to their low electronic noise, the calorimeters will also provide a pure and efficient interaction trigger when the LHC will start. All expected triggers from the calorimeter system will be ready to be registered in pass through mode from the start of the LHC in order to get to the standard configuration as soon as possible.

References

- [1] Antunes Nobrega R *et al.* (LHCb Collaboration) 2003 LHCb Reoptimized Detector Design and Performance Technical Design Report *CERN-LHCC-2003-030*
- [2] Amato S *et al.* (LHCb Collaboration) 2000 LHCb Calorimeters Technical Design Report *CERN-LHCC-2000-036*
- [3] Antunes Nobrega R *et al.* (LHCb Collaboration) 2003 LHCb Trigger System Technical Design Report *CERN-LHCC-2003-031*
- [4] Gaspar C, Jacobsson R, Jost B, Morlini S, Neufeld N, Vannerem P and Franek B 2004 An integrated experiment control system, architecture, and benefits: the LHCb approach *IEEE Trans. Nucl. Sci.* **51** 513
- [5] Guzik Z, Jacobsson R, Jost B 2004 Driving the LHCb front-end readout *IEEE Trans. Nucl. Sci.* **51** 508
- [6] Deschamps O, Machefert F, Schune M H, Pakhlova G and Belyaev I 2003 Photon and neutral pion reconstruction *LHCB-2003-091*
- [7] Shchutska L, Golutvin A and Belyaev I 2007 Study of radiative penguin decays $B^0 \rightarrow K^{*0}\gamma$ and $B_s^0 \rightarrow \phi\gamma$ at LHCb *CERN-LHCB-2007-030*
- [8] Breton V, Brun N and Perret P 2001 A clustering algorithm for the LHCb electromagnetic calorimeter using a cellular automaton *LHCB-2001-123*
- [9] Deschamps O, Monteil S, Perret P, Robert A, Machefert F, Robbe P and Schune M H 2007 The CKM angle α at LHCb *CERN-LHCB-2007-046*
- [10] Snyder A E and Quinn H R 1993 Measuring CP asymmetry in $B \rightarrow \rho\pi$ decays without ambiguities *Phys. Rev. D* **48** 2139